SRR-88-02

Observed Behaviour of a New Medium Span Slab-on-Girder Bridge

Ontario
Ministry of Transportation
Research and Development Branch

89-03145

Technical Report Documentation Page

Observed Behaviour of a New Medium Span Slab-on-Girder Bridge

Author(s):	B. Bakht, Principal Research Officer Structures Research Office, Research and Development Branch
Number:	SRR-88-02
Date of Publication:	June, 1988
Ministry Contact:	Baidar Bakht (416) 235-4674
Abstract:	This report relates to a behaviour test on a relatively new slab-on-girder bridge called the North Muskoka River bridge. The bridge, which has a span of 45.7 m, consists of five steel plate girders and a composite concrete deck slab. The apparently simply-supported girders rest on elastomeric bearings. The test on the North Muskoka River Bridge was conducted to establish the reasons why this particular bridge, like others of its kind, appeared flexurally stiffer in a previous test than could be rationalized analytically. The test data confirmed that the elastomeric bearings of the bridge provided enough horizontal restraint to the movement of the bottom flanges of the girders to reduce the applied live load moments by a minimum of 9%. This report provides all the relevant test data and their analysis.
Comments:	
Key words:	bearing restraint, composite action, elastomeric bearings, evaluation, load distribution, slab-on-girder bridge, bridge testing
Distribution:	MTO Head Office and Regions, selected structural engineers around the world, and upon request.
Copyright Status:	Crown copyright © 1988 Ministry of Transportation

SRR-88-02

Observed Behaviour of a New Medium Span Slab-on-Girder Bridge

B. Bakht
Principal Research Officer
Structures Research Office
Research and Development Branch

Published by
The Research and Development Branch
Ministry of Transportation, Ontario
Hon. Ed Fulton, Minister
D.G. Hobbs, Deputy Minister

Published without prejudice as to the application of the findings.
Crown copyright reserved; however, this document may be reproduced for non-commercial purposes with attribution to the Ministry.

For additional copies, contact:
The Editor, Technical Publications
Room 320, Central Building
1201 Wilson Avenue
Downsview, Ontario
Canada M3M 1J8

Telephone: (416) 235-3480
CNCP Dialcom Electronic Mail: 23:MIN006

June 1988

Table of Contents

1/ Test Summary 1

2/ Reasons for Test 2

3/ Bridge Description 3

4/ Details of Instrumentation and Test 4
4.1/ Instrumentation 4
4.2/ Test Loads 4

5/ Recorded Data 5

6/ Discussion of Results 6
6.1/ Checking of the Data 6
6.2/ Bearing Restraint 6
6.3/ Calculation of Girder Moments from Measured Strains 7
Beneficial Effect of Bearing Restraint 9
Examples of Calculation 10
Comparison with Beam Moments 12
6.4/ Lateral Distribution 13
Comparison with Analytical Results 14

7/ Conclusions 15

References 16

1/ Test Summary

Bridge:	North Muskoka River bridge (northbound) on Highway 11, MTC Site No. 42-58.
Type of Bridge:	Single span slab-on-girder bridge with steel plate girders and composite concrete slab.
Posting:	None
Span/Width:	45.72/14.62 m
Angle of Skew:	0°
Date of Test:	June 26, 1986
Test Engineer:	Baidar Bakht
Job Captain:	Zdislaw Knobel
Supervisor, Instrumentation:	Bill Kwok
Maximum Load Applied:	Two vehicles, each weighing about 650 kN (67 t)
Responses Monitored:	Strains in all girders at mid-span and near supports, and mid-span deflections of girders.
Conclusions:	In spite of being relatively new, the neoprene bearings provided enough restraint to the girders to reduce the live load moments by about 10%.

2/ Reasons for Test

Many tests on slab-on-girder bridges conducted in Ontario and the U.S.A. have led to the conclusion that these bridges are much stiffer than shown by calculations. Billing (1984) tested the North Muskoka River bridge in Ontario to determine its dynamic characteristics; he observed that the longitudinal flexural rigidity of the bridge was much larger than could be rationalized analytically. In an attempt to find the reason for the discrepancy, this bridge (which is described in Section 3 of this report) was analysed by the grillage analogy method, which can take account of the variations of the girder moment of inertia along its length. All those factors which could have enhanced the longitudinal flexural rigidity of the bridge were incorporated in the analysis. These factors included the stiffening effects of the barrier walls and horizontal wind bracing, and the adoption of a low value of 6.5 for the modular ratio of steel to concrete.

It was found that the patterns of transverse distributions of predicted and observed deflections were similar; however, their sums, which are statically determinate in single-span right bridges with truly simply-supported ends,were found to be only about 80% of the predicted ones. The test which is described in this report was undertaken to find the reasons for this apparent discrepancy. Most of the relevant data obtained during the test are recorded herein, as is the analysis of the data.

3/ Bridge Description

The North Muskoka River bridge is a simply-supported, single-span slab-on-girder bridge with zero angle of skew; it has five steel plate girders of constant depth and a composite concrete deck slab. The span and width of the bridge are 45.72 m and 14.62 m, respectively. The bridge is relatively new, being about 13 years old at the time of the test.

Some relevant details of the bridge are shown in Figure 3.1. As shown in this figure, the deck slab is about 200 mm thick. The deck also has two curbs and monolithic concrete barrier walls. The girder webs are of constant depth and thickness, but each flange has three different cross-sections, as shown in Figure 3.1.

Each end of every girder rests on a laminated neoprene bearing measuring 560 x 355 mm in plan and 64 mm in thickness. The design shear rate for each bearing was about 30 kN/mm. At the time of the test, the bearings were found to be in excellent condition.

4/ Details of Instrumentation and Test

4.1/ Instrumentation

All girders were instrumented with strain gauges to measure longitudinal strains at three different transverse sections, with one section near the mid-span and each of the other two near an abutment. Electrical resistance strain gauges were used at the top flanges and webs, and demountable strain transducers were attached to the bottom flanges. Deflections of the girders at mid-span were measured by deflection transducers. The locations of the various instruments are shown in Figure 4.1 together with their identifying numbers.

4.2/ Test Loads

The two Ministry test vehicles were used to test the bridge. Axle loads and spacings of these vehicles corresponding to the three load levels used in the test are shown in Figure 4.2. It is noted that, consistent with normal commercial vehicles, the centres of the two lines of wheels of the test vehicles are 1.83 m apart.

The bridge was tested with a single test vehicle in each of four different transverse positions, and also with both vehicles in one eccentric transverse position. For each transverse position, the vehicle, or vehicles, were placed at six different locations along the bridge. These transverse and longitudinal positions of the test vehicles are shown in Figure 4.3. The vehicles were brought onto the bridge at crawling speed, and the readings of the instruments were recorded a few seconds after the vehicle, or vehicles, had been brought to a halt at the stated positions on the bridge.

5/ Recorded Data

The girder strains and deflections were the largest when the test vehicles were in longitudinal position number 4, which is identified in Figure 4.3. Consequently, only the test data corresponding to this longitudinal position of the vehicles are recorded in this report.

Longitudinal strains in the various girders at mid-span due to vehicles in different locations and with the three load levels are listed in Table 5.1. The bottom flanges of three girders were instrumented at the mid-span by two demountable strain transducers with one close to each edge of the flange. Readings from these pairs of transducers are separated by a slash in Table 5.1.

Girder strain data for the two instrumented sections near the abutments, due to load level 3, are recorded in Table 5.2, and girder deflections at mid-span in Table 5.3. Girder deflections at the mid-span are plotted in Figure 5.1 for various load cases.

6/ Discussion of the Results

6.1/ Checking of the Data

One of the ways to establish whether the instruments are working properly is to perform a summation check on the measured responses. In such a check, the sums of responses due to two separate load cases are compared with their counterparts due to a load case which is formed by superposing the two load cases. As can be seen in Figure 4.3, vehicles in transverse position, or line, Nos. 2 and 3 constitute the former two load cases, and those in transverse position No. 4 the latter. It may be noted that a summation check is valid only for those structures whose behaviour is linear and elastic, in accordance with the principle of superposition.

Summation checks on a random selection of measured responses confirmed that the readings were reliable. A selection of the summation checks is given in Table 6.1.

As discussed later, the strains in the bottom flanges of girders near the bearings were unexpectedly large. These strains were thoroughly checked for repeatability and for the consistency of pattern. In addition, it was confirmed, as shown in Table 6.2, that for a given girder and load case, the bottom flange strains near the two bearings were very nearly the same.

6.2/ Bearing Restraint

The North Muskoka River bridge is simply supported with a single right span. If the neoprene bearings had permitted a free longitudinal movement of the girders, then under live loads the strains of the bottom flange near the bearings would have been tensile and very small. As can be seen in Tables 5.1 and 6.2, this is not the case. The vehicle loads induced fairly large compressive strains in the bottom flanges near the bearings.

A typical observed strain distribution over the girder depth near a bearing is shown in Figure 6.1. To obtain the net strains due to the bearing restraint force, the strains due to pure bending of the girders should be subtracted from the observed strains. However, the bending strains at the instrumented sections, which are very close to the bearings, are expected to be small, being of the order of 6 $\mu\varepsilon$ for level 3 loads even after accounting for the non-linear distribution of bending strains. A typical distribution of net strains due to the bearing restraint force is shown in Figure

6.1. As shown in this figure, the compressive strains are limited to the bottom flange and a relatively small part of the web. Therefore, the bearing restraint force can be obtained approximately by multiplying the stress due to observed bottom flange strain near the bearings by the cross-sectional area of the bottom flange. Such an approximation is done with the knowledge that it would lead to computed bearing restraint forces somewhat smaller than the actual ones.

The bearing restraint forces calculated according to this procedure are plotted in Figure 6.2 for vehicles with two different load levels in longitudinal position No. 4 (which is identified in Figure 4.3). It may be noted that the bearing restraint forces corresponding to different girders are joined by continuous curves to facilitate readability.

The patterns of transverse distribution of bearing restraint forces due to vehicles in given positions were found to be similar for different load levels, thus further confirming the reliability of the measured data.

Bearing restraint forces of the order of 175 kN, which can be seen from Figure 6.2, are larger than a functioning neoprene bearing can be expected to develop. Nevertheless, such large forces were, indeed, present. A further proof of the presence of large bearing restraint forces was provided by a comparison of applied moments with those computed from girder strains.

6.3/ Calculation of Girder Moments from Measured Strains

In the absence of bearing restraint forces, the total moment taken by a composite girder can be divided into M_L, M_u and Na, where, as shown in Figure 6.3(a), M_L is the moment taken by the naked steel girder flexing about its own neutral axis; M_u is the moment taken by the concrete flange acting about its own neutral axis; N is the axial force acting in opposite directions in the steel girder and the concrete flange; and a is the lever arm for the two equal and opposite axial forces. Thus, the moment M taken by the composite girder is given by:

$$M = M_L + M_u + Na \qquad (6.1)$$

When there is no axial force in the girder due to bearing restraint, then, as shown in Figure 6.3(b), the girder stresses, which are obtained by multiplying strains with the modulus of elasticity of steel, can be readily separated into stresses due to pure flexure and those due to the axial force N.

From the stresses thus separated the various components of Equation 6.1 can be calculated as follows:

$$M_L = \sigma_{fb} S_b \quad (6.2)$$

$$M_u = M_L (EI_s/EI_g) \quad (6.3)$$

$$Na = \sigma_a Aa \quad (6.4)$$

where,

σ_{fb} = stress in the bottom flange o the steel girder due to pure flexure

S_b = section modulus of the naked steel girder with respect to the bottom flange

EI_s = flexural rigidity of the associated portion of the concrete slab bending about its own neutral axis.

EI_g = flexural rigidity of the naked steel girder bending about its own neutral axis

σ_a = axial stress in the naked steel girder due to axial force N.

A = area of cross-section of the naked steel girder

a = lever arm of the couple due to axial forces N

In the absence of net axial force in the girder due to bearing restraint, the lever arm a is approximately equal to the distance between the neutral axes of the concrete slab and the naked steel girder.

The expressions given about are clearly based on the assumption that plane sections remain plane, i.e., that the strain distribution over the entire depth of the beam remains linear, in which case the value of total moment M taken by the composite girder at a particular section can be determined fairly accurately from only two strain readings over the depth of the girder at the section under consideration. It is noted that the value of E for steel remains fairly constant at approximately 200 MPa. The modulus of elasticity of concrete has little influence on M, since the only quantity affected by this modulus of elasticity is M_u which is always very small as compared to M_L and Na.

Equations 6.1 through 6.4 are valid only if the section is free from axial forces due to bearing restraint. As discussed in Section 6.2, and observed in several tests, slab-on-girder bridges are rarely free from bearing restraint. It follows, therefore, that the values of σ_t and σ_b, i.e., the top and bottom girder stresses, respectively, due to applied moment only should be obtained by

subtracting the effect of bearing restraint from stresses computed from measured strains. This can be done as follows.

Let the stresses computed from observed strains in the top and bottom flanges of the girder at the section under consideration be designed as σ_t' and σ_b' respectively; and the stress computed from the observed strain at the bottom flange near a bearing be designated as σ_s'. As mentioned earlier, the axial force F, due to bearing restraint can be approximately given by:

$$F = \sigma_s' A_f \tag{6.5}$$

where A_f is the area of the bottom flange at the instrumented section near a bearing. The average axial stress σ_{as} due to bearing restraint can be obtained from;

$$\sigma_{as} = \frac{F}{A_c} \tag{6.6}$$

where A_c is the equivalent area of the cross-section of the composite girder. It is noted that the value of the modulus of elasticity of concrete may have a significant influence on A_c, and therefore on σ_b.

The values of σ_t and σ_b can now be obtained from:

$$\sigma_t = \sigma_t' - \sigma_{as} \tag{6.7}$$

$$\sigma_b = \sigma_b' - \sigma_{as} \tag{6.8}$$

The above process of obtaining stresses due to flexure from stresses computed from measured strains, is illustrated in Figure 6.3(c). It is noted that the moments obtained from σ_t and σ_b from Equations 6.2 to 6.3 correspond to the neutral axis location of the composite section.

Beneficial Effect of Bearing Restraint

The net effect of the forces developed due to bearing restraint is to reduce the applied moment and to stiffen the girders flexurally. The analytical treatment of the effects of bearing restraint is given by Bakht and Jaeger (1988). However, with the help of Figure 6.4, it can be readily appreciated that the bearing restraint force F induces a moment in the opposite sense of that caused by the applied loads. This moment at the neutral axis is equal to $F\bar{y}$ where $\bar{y}$ is the vertical distance

between the neutral axis of the composite girder at the section under consideration, and the middle of the bottom flange. If $\bar{y}$ is calculated from measured strains, then care should be exercised in first discounting the axial strains due to F, and then determining the value of $\bar{y}$.

Examples of Calculation

The cross-sectional properties of a typical girder of the North Madawaska River bridge at the mid-span and near one of the abutments are shown in Figure 6.5. Only those properties are noted in this figure which will be utilized in the calculation of moments taken by the composite girder.

The example of calculations given below is for moments in girder D due to the test vehicle at load level 3 (see Figure 4.2) in transverse position No. 1 and longitudinal position No. 4. As can be seen from Table 5.1, the strain ε_t at mid-span at the top flange is $-20\mu\varepsilon$ and the strain ε_b in the bottom flange at web location is $126\mu\varepsilon$ [= (130 + 121)/2]; and the web strain at mid-height is $50\mu\varepsilon$. As shown in Table 5.2, the bottom flange strain ε_s due to the same loading is $-15\mu\varepsilon$ at one end and $-18\mu\varepsilon$ at the other with the average of $-16\mu\varepsilon$, with the compressive strains shown as –ve and tensile as +ve. It is readily confirmed that the strains at the mid-span are very nearly linear over the depth of the girder.

Assuming a modular ratio of 8, the transformed cross-sectional area of the composite girder at the mid-span is found to be 0.133 m^2 in steel units.

Bearing restraint force $F = -16 \times 10^{-6} \times 0.0174 \times 2 \times 10^8 = -55.7$ kN

$\sigma_{as} = -(55.7/0.133) = -419$ kN/m^2

$\sigma_t = -20 \times 10^{-6} \times 2 \times 10^8 - (-419) = -3581$ kN/m^2

$\sigma_b = 126 \times 10^{-6} \times 2 \times 10^8 - (-419) = 25{,}619$ kN/m^2

$$\bar{y} = \frac{2.19}{1 - (-3581/25619)} = 1.92 \text{ m}$$

Recognizing that the neutral axis of the steel girder is 0.973 m above the middle of the bottom flange, it can be shown that:

$$\sigma_{fb} = \frac{\sigma_f - \sigma_t}{2.255}$$

$$\sigma_a = \frac{F_t + 1.225\sigma_b}{2.255}$$

so that

$$\sigma_{fb} = \frac{25619 + 3581}{2.255} = 12{,}949 \text{ kN/m}^2$$

$$\sigma_a = \frac{-3581 + 1.255 \times 25619}{2.255} = 12{,}670 \text{ kN/m}^2$$

from σ_{fb}, M_L is given by:

$$M_L = 12{,}949 \times 0.0523 = 677 \text{ kN m}$$

The ratio of the flexural rigidities of the steel girder and 2.97 m wide deck slab about their respective neutral axes, is 195.9. Therefore:

$$M_u = \frac{677}{195.9} = 3 \text{ kN m}$$

The axial force N is obtained from σ_a:

$$N = 12670 \times 0.0586 = 742.5 \text{ kN}$$

The lever arm a, between the neutral axes of the girder and concrete flange is equal to 1.322 m. Hence, the couping moment Na:

$$Na = 742.5 \times 1.322 = 982 \text{ kN}$$

It is noted that a is equal to 1.322 m for internal girders, but for external girders in which the concrete flange also comprises the sidewalk and the barrier wall, its value is equal to 1.399 m.

The total moment M taken by the girder is the sum of M_L, M_u and Na.

$$M = 677 + 3 + 982 = 1662 \text{ N}$$

The moment due to the bearing restraint force at the neutral axis is $F\bar{y}$:

$$F\bar{y} = -55.7 \times 1.92 = -107 \text{ kN m}$$

It is obvious that the moment due to the applied load accepted by the girder is reduced by 107 kN m.

Comparison with Beam Moments

For the load case under consideration, the girder moments obtained by the above procedure are listed in Table 6.3, along with the values of $\bar{y}$ and $F\bar{y}$ for each girder. The table also contains the values of girder moments and $\bar{y}$ as they would be if the effects due to the bearing restraint are ignored, as they usually are.

The positions of the axles of the two test vehicles along the bridge span are shown in Figure 6.6 together with the total beam moments due to each vehicle at load levels 1 and 3. If the force F due to the bearing restraint were absent, the sum of girder moments computed from measured strains would be the same as the corresponding beam moment. From Table 6.3, it can be seen that the sum of girder moments at the mid-span obtained by ignoring the bearing restraint is 5258 kN m, being about 15% less the beam moment of 6202 kN m.

When the bearing restraint effects are taken into account, the sum of calculated moments at the mid-span becomes 5424 kN, as shown in Table 6.3. This moment is 5% less than the discounted beam moment of 5710 kN m which is obtained by subtracting the moments due to the bearing restraint forces from the beam moments.

Tables similar to 6.3 are given in Tables 6.4 through 6.6 for three other load cases and the comparisons of the beam moments at the mid-span with the sum of corresponding moments computed from measured strains by both including and ignoring the effects of bearing restraint are given in Table 6.7.

It can be seen in Table 6.7 that when bearing effects are ignored, the sums of computed moments are from 15 to 19% less than the corresponding beam moments.

It can also be seen in Table 6.7 that the bearing restraint in the north Madawaska River bridge has the effect of reducing the live load moments by a minimum of 9%. The sums of girder moments computed from measured strains by including the effects of bearing restraint are found to be in much closer agreement with the beam moments which are discounted for moments due to bearing restraint forces, with the difference ranging between –6 and +1%. A difference in this range could well have been caused by very small errors in measurements of strains and by the assumptions implicit in the calculations of the bearing restraint forces.

6.4/ Lateral Distribution

Mid-span girder moments computed by the procedure given above, are plotted in Figure 6.7 for two different load cases, each with vehicles at load levels 1 and 3. From these plots, the D values for moments can be readily calculated as follows, it being noted that D, which has units of length, is used in the Ontario and AASHTO codes as a measure of transverse load distribution. According to the methods of analysis given in these codes, the maximum girder moment, M_g, is given by:

$$M_g = \frac{Sm}{D} \qquad (6.9)$$

where S is the girder spacing and m is the moment due to one line of wheels of the vehicle. From Equation 6.9, it follows that:

$$D = \frac{Sm}{M_g} \qquad (6.10)$$

M_g is the maximum girder moment, which is computed from the strains, taking account of the bearing restraint force, and m is the sum of the similarly computed girder moments divided by the number of lines of wheels in the load case under consideration.

For the four cases for which moments are plotted in Figure 6.7, the values of D are calculated by Equation 6.10 with the steps of calculation and these resulting D values listed in Table 6.8(a).

It is also usual to use the bottom flange strains for calculating the D values. For such calculations Equation 6.10 can be modified as follows:

$$D = \frac{S}{n} \frac{\sum \varepsilon}{\varepsilon_{max}} \qquad (6.11)$$

where $\sum\varepsilon$ is the sum of all bottom girder strains at the transverse section under consideration, n is the number of lines of wheels in the load case, and ε_{max} is the maximum girder strain. For the same load cases which are dealt with the Table 6.8(a), the D values are recalculated from bottom flange strains. The steps of calculation and the resulting D values are given in Table 6.8(b). It is worthy of note that the two procedures do not give identical values, clearly because in the presence of bearing restraint forces the bottom flange strains no longer remain directly proportional to the girder moments. The maximum difference between the D values obtained by the two procedures is about 7%.

It is interesting to note that the D value for a particular load position may also vary with the load level, as can be seen in both Table 6.8(a) and Table 6.8(b). However, such variation is relatively small, being a maximum of 4% for the cases studied.

The positions of the flexural neutral axes of the composite girders were found to vary with both the vehicle positions and load levels. As shown in Figure 6.7, the positions of the neutral axes seem to reach a more or less common level only when they carry substantially heavy loads.

Comparison with Analytical Results

The North Muskoka River Bridge was analysed for some of test load cases by the grillage analogy method, in which the effects of bearing restraint cannot be included explicitly.

Girder moments at mid-span obtained from grillage analysis for two load cases are compared in Figure 6.8 with those computed from measured strains. These comparisons confirm yet again that the sum of the moments computed from measured data is much small than the sum of grillage moments. The pattern of transverse distribution of moments is, however, identical for the two sets of moments.

7/ Conclusions

It has been shown that at the time of the test in June, the mid-span moments in the North Muskoka River bridge due to vehicle loads were reduced by nearly 9% due to the bearing restraint forces. From the procedure given by Bakht and Jaeger (1988), it can be readily shown that such a reduction of mid-span moments would correspond to a reduction of about 12% in the mid-span deflections. However, the observed reduction of mid-span deflection in the test by Billing (1984) was of the order of 20%. This apparent discrepancy from the postulation that these reductions are caused by the bearing restraint forces, can be explained as follows.

The test reported herein was conducted on a very hot day in June, while the test by Billing was conducted in October on a relatively cold day. It is hypothesized that the neoprene bearings become stiffer with the drop of temperature, thereby providing a higher bearing restraint force in the colder temperature, which consequently results in a larger reduction of the load effects. It is probable, therefore, that the reduction of mid-span deflection in the October 1980 test was indeed caused by the restraint of bearings, which were stiffer at the time of that test than at the time of the June 1986 test.

There is clearly much to be learnt about the behaviour of neoprene bearings with regard to short-term low strains, especially if their beneficial action is to be included in the calculations for design and evaluation. However, the detrimental effect of these bearings causing unexpected lateral forces in piers and abutments should be taken into design consideration immediately.

References

[1] Bakht, B. and Jaeger, L.G. (1988). Support restraint in slab-on-girder bridges. To be published.

[2] Billing, J.R. (1984). Dynamic loading and testing of bridges in Ontario. *Canadian Journal of Civil Engineering*, Vol. 11, No. 4, pp. 833-843.

Table 5.1/ Longitudinal Strains in Girders at Mid-Span

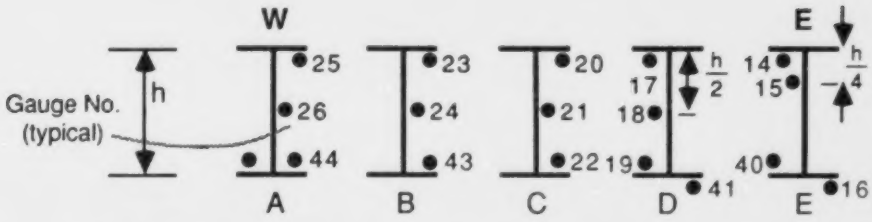

Load Level	Line Number	Position Number	Location on Girder	Strains x 10^6 at: Girder A	Girder B	Girder C	Girder D	Girder E
1	1	4	top flange	-3	-2	12	-13	-4
			web	4	8	28	33	23
			bottom flange	16/3	21	53/51	82/81	95/11
2	1	4	top flange	-3	-1	14	-14	-4
			web	4	14	7	43	29
			bottom flange	2	23	64	106/102	114/140
3	1	4	top flange	-6	-5	13	-20	-6
			web	4	13	38	50	40
			bottom flange	4	29	78/76	130/121	139/168
1	2	4	top flange	-6	10	-1	4	-4
			web	23	32	29	23	8
			bottom flange	56/27	50	66/69	54/52	40/65
2	2	4	top flange	-5	16	-9	6	-5
			web	33	35	29	30	9
			bottom flange	34	63	81/90	68/64	44/78
3	2	4	top flange	-7	14	-5	4	-6
			web	40	44	47	37	14
			bottom flange	40	75	97/109	86/77	54/97
1	3	4	top flange	-2	-7	3	-20	-8
			web	0	7	25	31	29
			bottom flange	-1	14	49/44	84/85	116/120
2	3	4	top flange	-1	-8	12	-21	-7
			web	0	9		38	36
			bottom flange	-2	18	61/58	109/107	140/152
3	3	4	top flange	-5	-12	10	-27	-11
			web	-2	9	36	47	48
			bottom flange	-3	21	73/67	132/129	172/183
1	4	4	top flange	-7	7	1	-7	-10
			web	27	37	30	56	40
			bottom flange	27	67	114/118	140/135	147/182
2	4	4	top flange	-8	9	1	-8	-13
			web	34	44		70	50
			bottom flange	32	82	142/151	182/170	181/232
3	4	4	top flange	-12	4	2	-14	-16
			web	37	52	95	87	68
			bottom flange	38	96	168/180	219/264	222/279
3	5	4	top flange	-7	-27	-30	-8	-5
			web	93	56	47	9	4
			bottom flange	110	126	83/84	33/42	8/28

Note: Compressive strain is shown as -ve.

Table 5.2/ Girder Strains Near Abutments due to Vehicles at Load Level 3 and Position 4

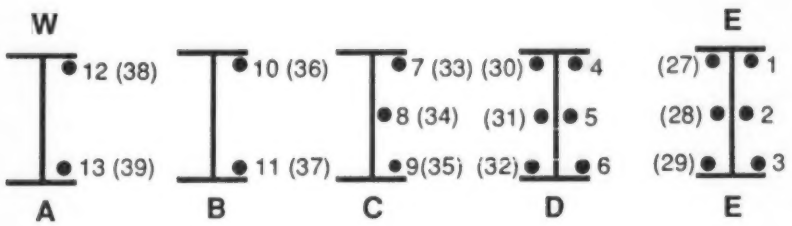

Line No.	Location on Girder	Strains x 10^6 at: Girder A	Girder B	Girder C	Girder D	Girder E
1	top flange	1 (0)	6 (0)	6 (5)	–1 (–4)	–1 (–4)
	web			5 (4)	5 (2)	9 (5)
	bottom flange	0 (0)	–4 (–3)	–16 (–13)	–15 (–18)	–30 (–30)
2	top flange	2 (0)	5 (0)	2 (2)	2 (–2)	1 (0)
	web			3 (0)	3 (0)	4 (4)
	bottom flange	–17 (–9)	–11 (–11)	–16 (–13)	–9 (–8)	–15 (–13)
3	top flange	1 (1)	6 (1)	7 (6)	–1 (–4)	–2 (–3)
	web			5 (6)	7 (6)	10 (8)
	bottom flange	–2 (0)	–3 (–2)	–14 (–14)	18 (–22)	–34 (–37)
4	top flange	–1 (–1)	13 (1)	11 (9)	0 (–1)	1 (–2)
	web			8 (8)	13 (6)	13 (12)
	bottom flange	–15 (–9)	–14 (–13)	–30 (–26)	–27 (–31)	–49 (–51)
5	top flange	0 (–1)	1 (–1)	0 (0)	4 (0)	1 (2)
	web			1 (–1)	–1 (–1)	1 (1)
	bottom flange	–37 (–21)	–16 (–20)	–14 (–10)	–2 (–1)	2 (0)

Note: Compressive strain is shown as –ve.

Table 5.3/ Girder Deflections at Mid-Span

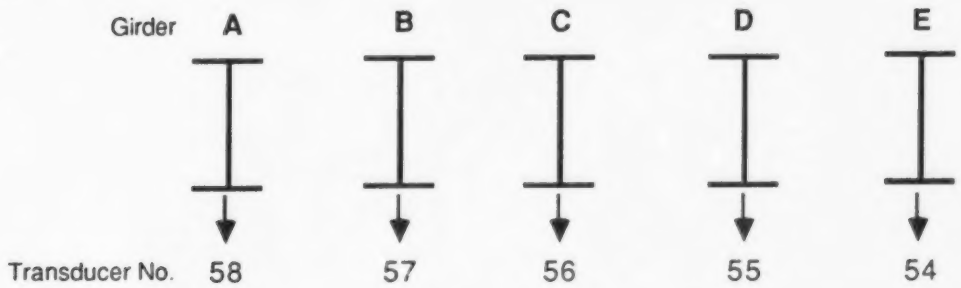

Load Level	Line Number	Position Number	Deflections in mm for: Girder A	Girder B	Girder C	Girder D	Girder E
1	1	4	1.1	3.4	6.3	9.2	7.7
2	1	4	1.6	4.6	8.0	11.8	9.8
3	1	4	1.9	5.0	9.3	13.9	11.5
1	2	4	5.2	6.4	7.6	6.9	4.2
2	2	4	6.2	8.1	9.0	8.2	4.9
3	2	4	7.9	9.6	11.4	10.4	6.5
1	3	4	0.1	2.6	5.5	9.0	8.6
2	3	4	0.8	3.9	7.5	12.1	11.0
3	3	4	0.7	4.3	9.2	14.3	12.8
1	4	4	5.8	9.5	13.2	15.9	12.1
2	4	4	7.3	11.8	16.7	20.5	15.1
3	4	4	8.6	14.1	20.4	24.9	18.1
3	5	4	15.6	13.1	9.1	5.4	1.9

Note: Downward deflection is known as +ve.

Table 6.1/ Summation Checks Corresponding to Load Level 3 and Longitudinal Position 4

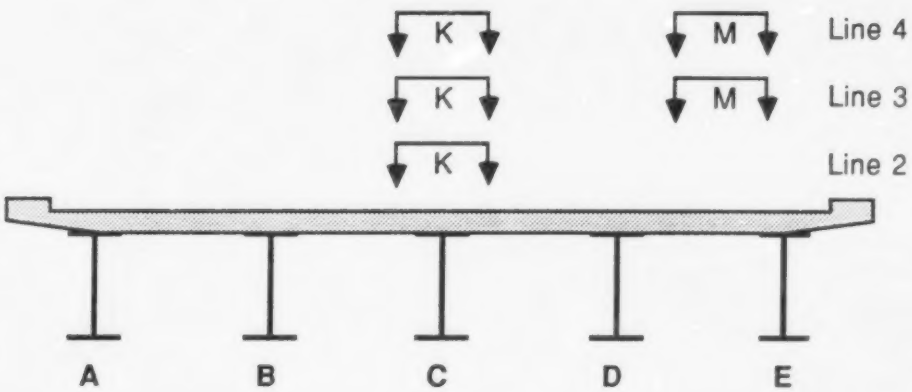

Instrumented Location	Vehicle Line Number	Strains x 10^6 at: Girder A	Girder B	Girder C	Girder D	Girder E
top flange at mid-span	2	–7	14	–5	4	–6
	3	–5	–12	10	–27	–11
	Σ(2+3)	–12	2	5	–23	–17
	4	–12	4	2	–14	–16
bottom flange at mid-span	2	40	75	103	81	76
	3	–3	21	70	130	178
	Σ(2+3)	37	96	173	211	254
	4	38	96	174	211	251
bottom flange near S. abutment	2	–17	–11	–16	–8	–15
	3	2	–3	–14	–18	–34
	Σ(2+3)	–15	–14	–30	–26	–49
	4	–15	–14	–30	–27	–49

Note: compressive strains are shown as –ve.

Table 6.2/ Longitudinal Strains in Bottom Flanges of Girders Near Supports

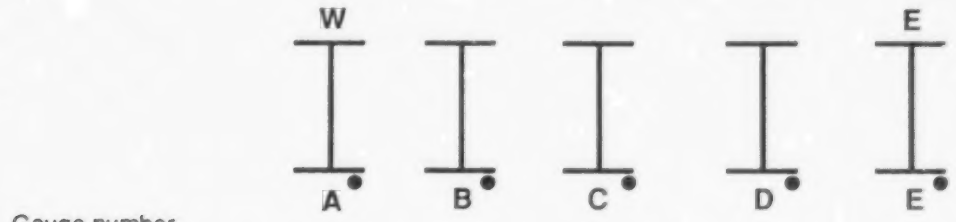

Load Level	Line Number	Position Number	Section	Strains x 10^6 at: Girder A	Girder B	Girder C	Girder D	Girder E
1	1	4	N	0	–1	–8	–13	–20
			S	0	–2	–13	–10	–20
2	1	4	N	–1	–4	–11	–17	–28
			S	–1	–5	–11	–14	–25
3	1	4	N	0	–3	–13	–18	–30
			S	0	–4	–16	–15	–30
1	2	4	N	–6	–6	–7	–7	–8
			S	–10	–6	–12	–6	–11
2	2	4	N	–7	–9	–11	–8	–12
			S	–14	–8	–10	–7	–12
3	2	4	N	–9	–11	–13	–9	–13
			S	–17	–11	–16	–8	–15
1	3	4	N	–1	–1	–9	–15	–26
			S	–1	–1	–5	–12	–21
2	3	4	N	0	–2	–13	–20	–32
			S	1	–3	–12	–16	–30
3	3	4	N	0	–2	–14	–22	–37
			S	2	–3	–14	–18	–34
1	4	4	N	–5	–8	–18	–21	–34
			S	–11	–9	–17	–18	–32
2	4	4	N	–10	–12	–25	–29	–46
			S	–13	–12	–21	–24	–42
3	4	4	N	–9	–13	–26	–31	–51
			S	–15	–14	–30	–27	–49

Note: compressive strains are shown as –ve.

Table 6.3/ Girder Moments at Mid-Span at the Neutral Axis due to Load Level 3, Line No. 1, and Longitudinal Position No. 4

Girder	Including Bearing Restraint			Ignoring Bearing Restraint Effects	
	Girder Moment (kN m)	$\bar{y}$ (m)	F $\bar{y}$ (kN m)	$\bar{y}$	Girder Moment (kN m)
A	41	0.89	0	0.88	41
B	384	1.92	–27	1.88	374
C	1093	2.74	–143	2.65	1054
D	1662	1.94	–107	1.90	1633
E	2244	2.19	–215	2.12	2156
Σ	5424		–492		5258

Net applied moment = 6202 – 492 = 5710 kN m

Table 6.4/ Girder Moments at Mid-Span at the Neutral Axis due to Load Level 1, Line No. 1, and Longitudinal Position No. 4

Girder	Including Bearing Restraint			Ignoring Bearing Restraint Effects	
	Girder Moment (kN m)	$\bar{y}$ (m)	F $\bar{y}$ (kN m)	$\bar{y}$	Girder Moment (kN m)
A	132	1.69	0	1.69	132
B	265	2.04	–15	2.03	261
C	742	2.97	–102	2.87	718
D	1090	1.95	–74	1.90	1085
E	1476	2.06	–144	2.13	1474
Σ	3705		–335		3670

Net applied moment = 4017 – 335 = 3682 kN m.

Table 6.5/ Girder Moments at Mid-Span at the Neutral Axis due to Load Level 3, Line No. 4 (Two Vehicles), and Longitudinal Position No. 4

Girder	Including Bearing Restraint			Ignoring Bearing Restraint Effects	
	Girder Moment (kN m)	$\bar{y}$ (m)	F $\bar{y}$ (kN m)	Girder Moment (kN m)	$\bar{y}$ (m)
A	574	2.34	105	449	1.67
B	1320	2.35	106	1287	2.30
C	2390	2.29	223	2322	2.23
D	2861	2.12	214	2791	2.08
E	3627	2.14	373	3499	2.07
Σ	10,772		1021	10,348	

Net applied moment = 6202 + 6224 – 1021 = 11,405.

Table 6.6/ Girder Moments at Mid-Span at the Neutral Axis due to Load Level 1, Line No. 4 (Two Vehicles), and Longitudinal Position No. 4

Girder	Including Bearing Restraint			Ignoring Bearing Restraint Effects	
	Girder Moment (kN m)	$\bar{y}$ (m)	F $\bar{y}$ (kN m)	Girder Moment (kN m)	$\bar{y}$ (m)
A	384	1.84	–51	363	1.75
B	911	2.34	–73	909	2.46
C	1590	2.28	–135	1548	2.22
D	1858	2.14	–150	1812	2.10
E	2378	2.15	–247	2166	2.08
Σ	7121		–656	6798	

Net applied moment = 4017 + 4057 – 656 = 7418 kN m

Table 6.7/ Comparison of Computed Mid-Span Moments at the Neutral Axis with Beam Moments

Load Level	Line Number	Long'l Position Number	M_{BEAM} (kN m)	ΣM_f (kN m)	$\frac{\Sigma M_f}{M_{BEAM}}$	M'_{BEAM} (kN m)	ΣM (kN m)	$\frac{\Sigma M}{M'_{BEAM}}$
3	1	4	6202	5258	0.85	5710	5424	0.95
1	1	4	4017	3670	0.91	3682	3705	1.01
3	4	4	12,426	10,348	0.83	11,405	10,772	0.94
1	4	4	8074	6798	0.84	7418	7121	0.96

M_{BEAM} = beam moment

M'_{BEAM} = beam moment less $\Sigma F \bar{y}$

ΣM_f = sum of girder moments computed from measured strains ignoring the effects of bearing restraint.

ΣM = sum of girder moments computed at the neutral axis from measured strains by taking account of the effects of bearing restraint.

Table 6.8/ Calculation of D Values for Moments at Mid-Span

(a) Calculation from computed moments

Load Case*	Number of Lines of Wheels	Sum of Girder Moments (kN m)	Maximum Girder Moment (kN m)	D (m)
3,1,4	2	5424	2244	3.59
1,1,4	2	3705	1476	3.73
3,4,4	4	10,772	3627	2.21
3,1,4	4	7121	2378	2.22

* load level, line number, longitudinal position number.

(b) Calculation from measured strains at bottom flanges

Load Case*	Number of Lines of Wheels	Sum of Bottom Flange Strains ($\times 10^{-6}$)	Maximum Bottom Flange Strain ($\times 10^{-6}$)	D (m)
3,1,4	2	269	103	3.87
1,1,4	2	390	154	3.76
3,4,4	4	512	165	2.30
3,1,4	4	772	251	2.28

* load level, line number, longitudinal position number.

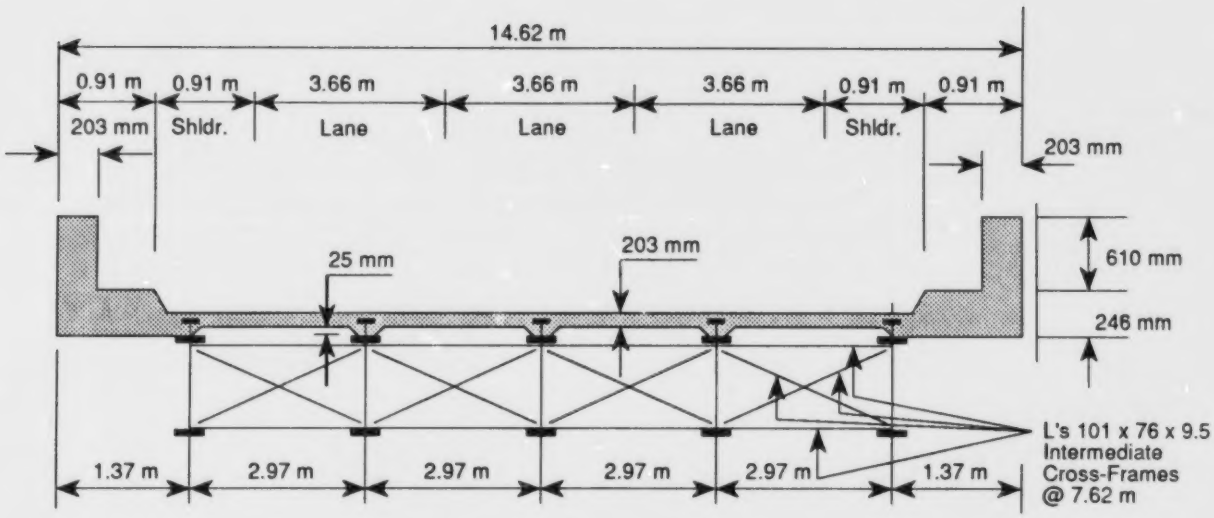

Cross-Section

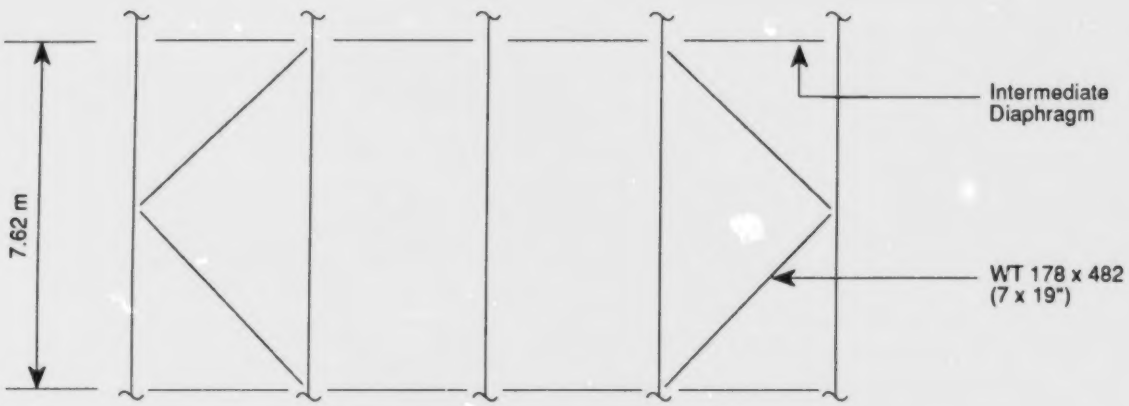

Part Plan Showing Horizontal Bracing

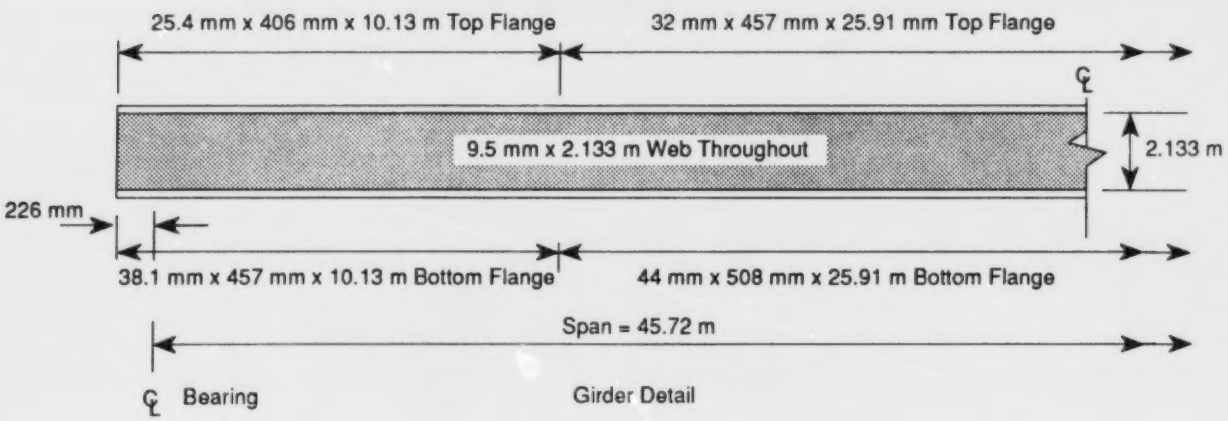
25.4 mm x 406 mm x 10.13 m Top Flange
32 mm x 457 mm x 25.91 mm Top Flange
9.5 mm x 2.133 m Web Throughout
2.133 m
226 mm
38.1 mm x 457 mm x 10.13 m Bottom Flange
44 mm x 508 mm x 25.91 m Bottom Flange
Span = 45.72 m
Bearing
Girder Detail

Figure 3.1/ Details of a Slab-on-Girder Bridge

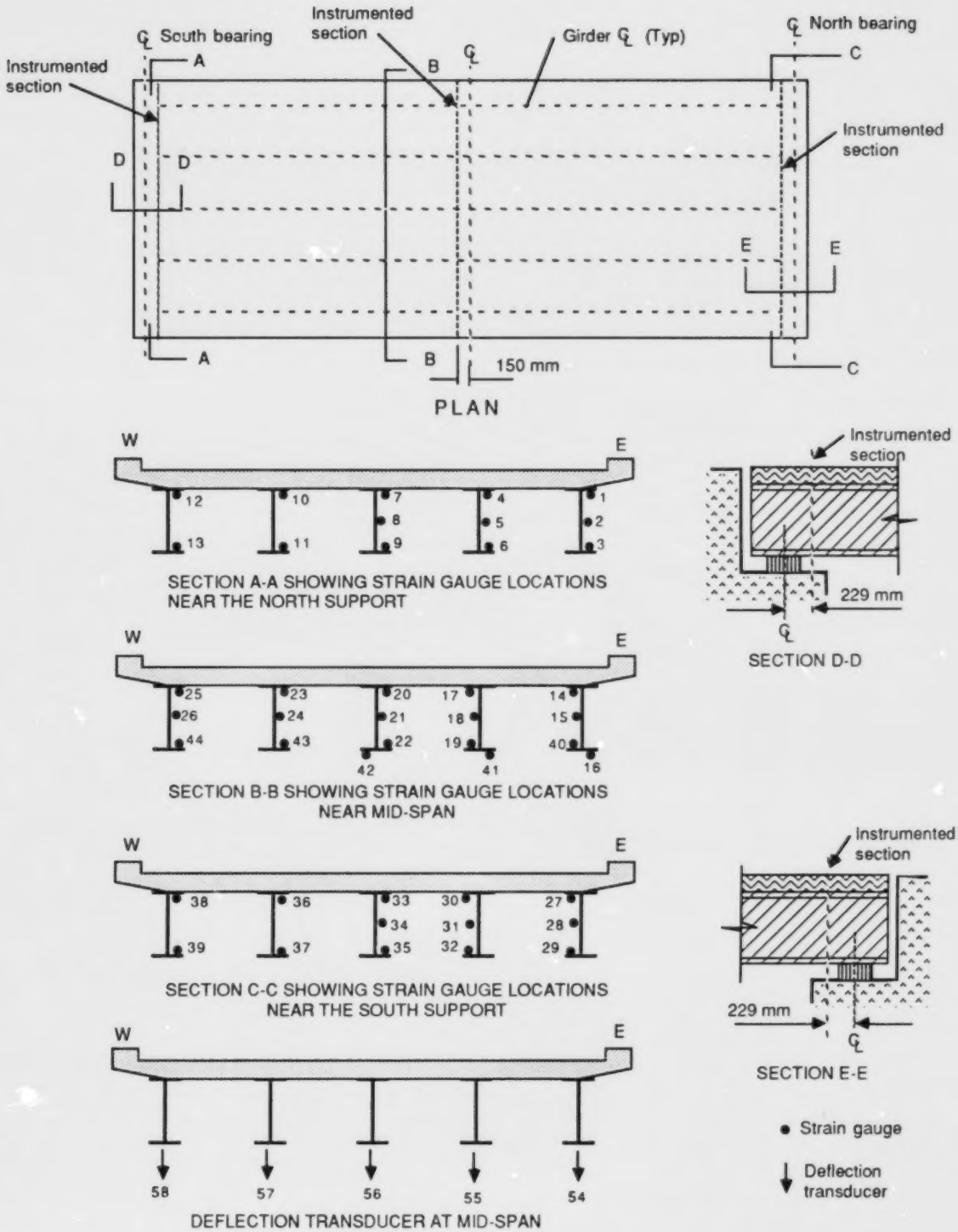

Figure 4.1/ Locations of Instruments and Their Identifying Numbers

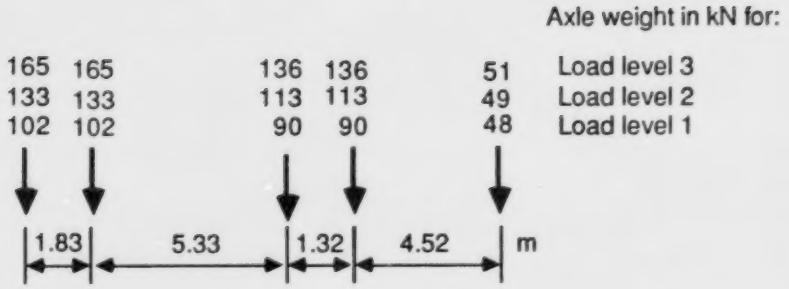

(a) Details of Kenworth vehicle

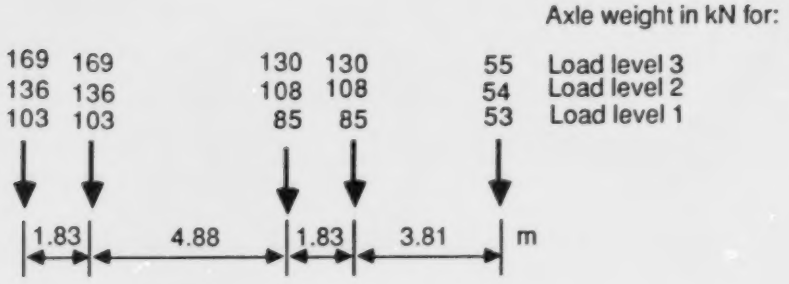

(b) Details of Mack vehicle

Figure 4.2/ Axle Weights and Spacings of the Test Vehicles

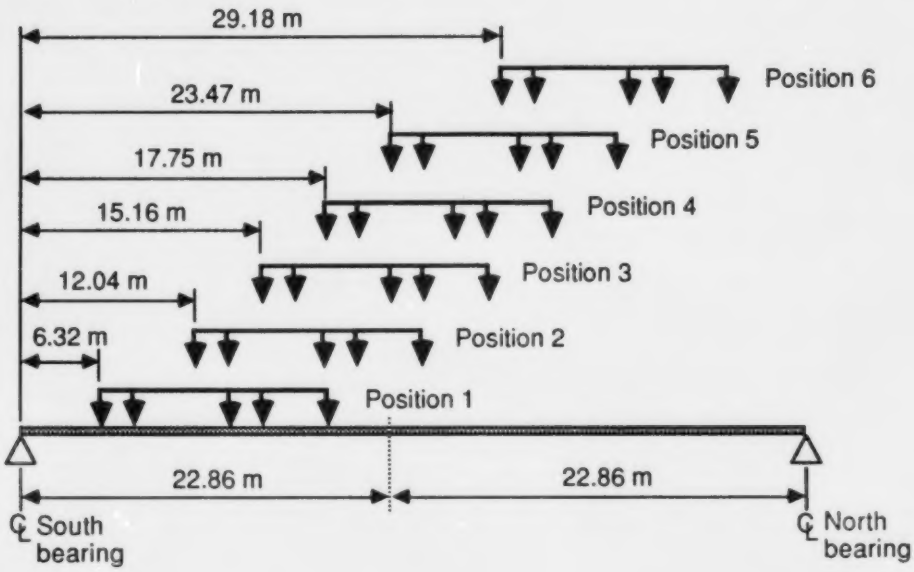

(a) Longitudinal vehicle positions

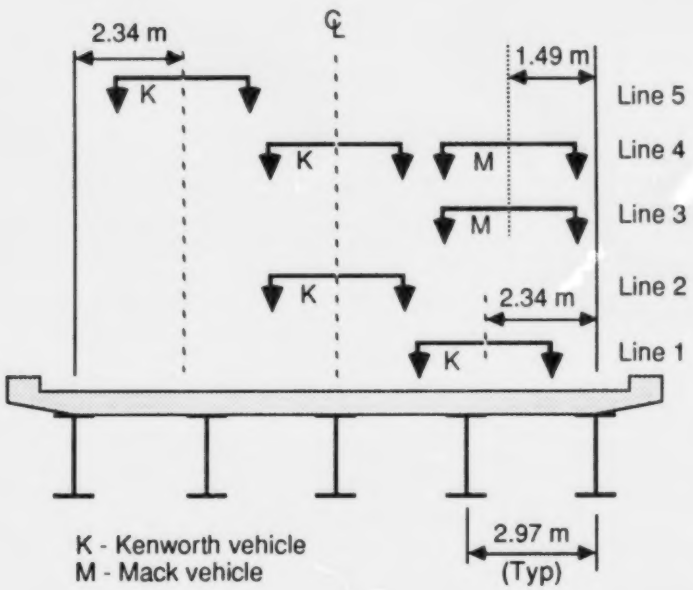

(b) Transverse vehicle positions

Figure 4.3/ Test Vehicle Positions and Their Identifying Numbers

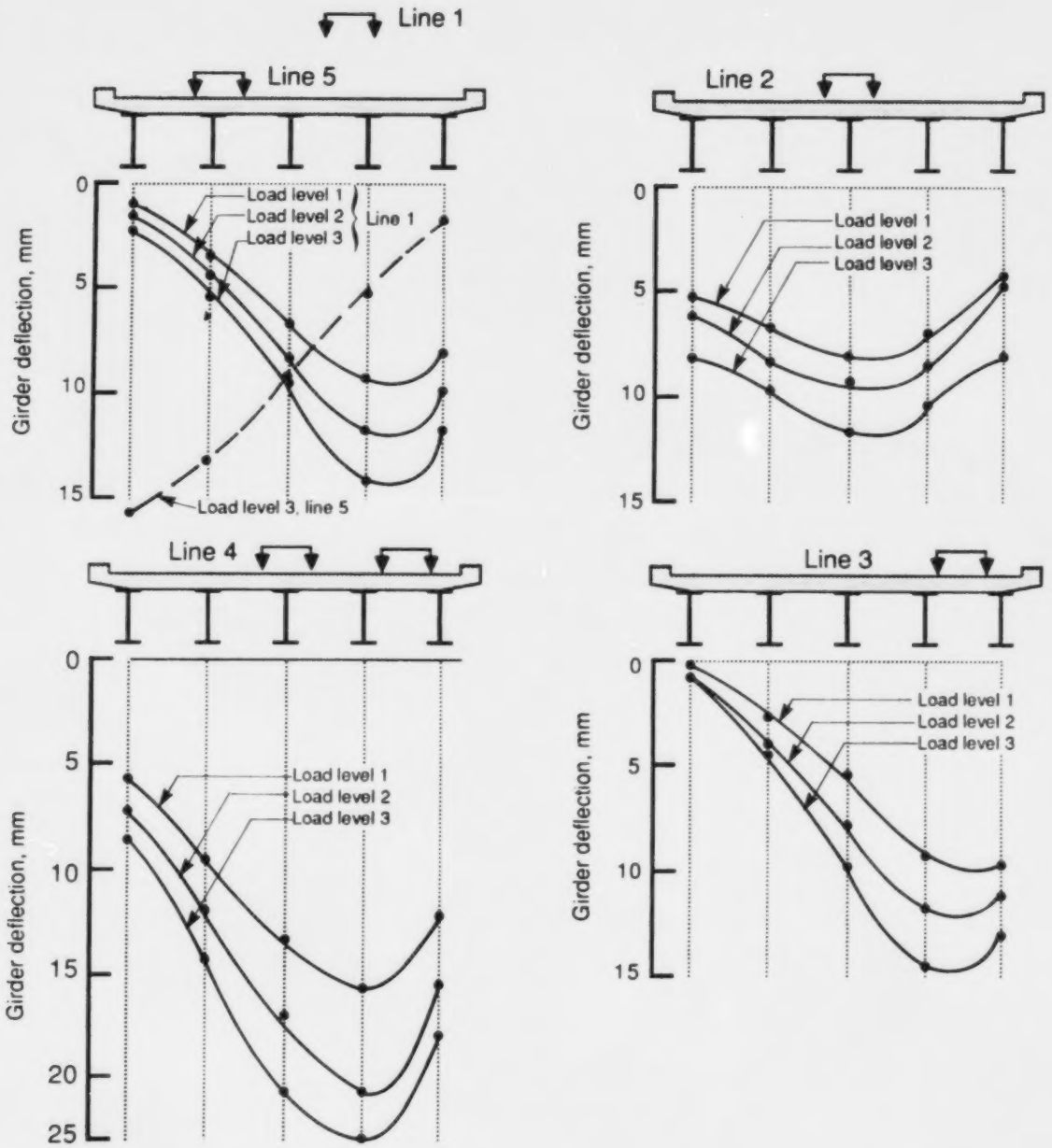

Figure 5.1/ Girder Deflections at Mid-Span for Load Position No. 4 (see Fig. 4.3)

Observed strain — Bending strain — Strain due to bearing restraint force

Figure 6.1/ Typical Strain Distribution Over Girder Depth Near an Abutment

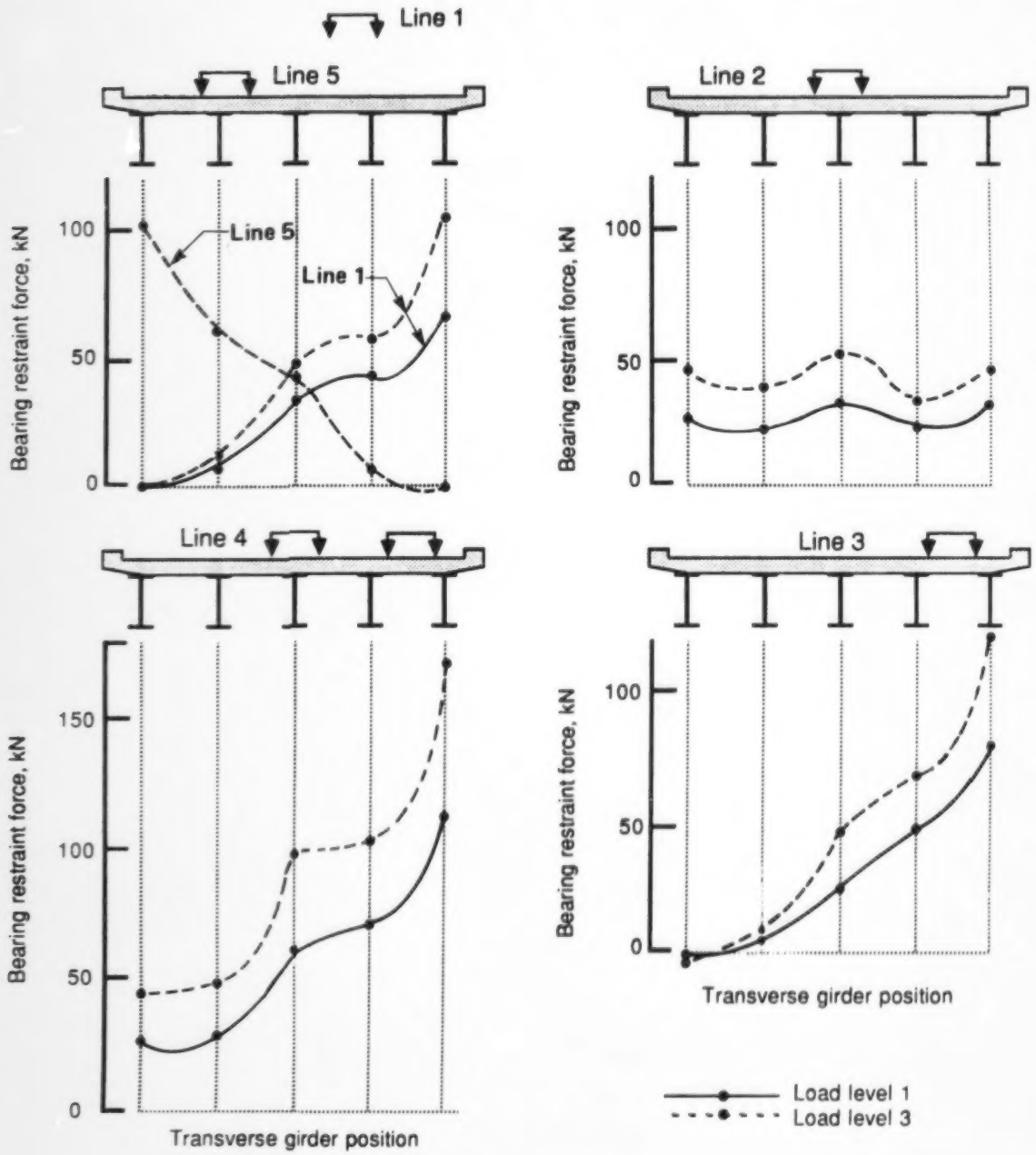

Figure 6.2/ Bearing Restraint Forces Corresponding to Vehicles in Longitudinal Position No. 4

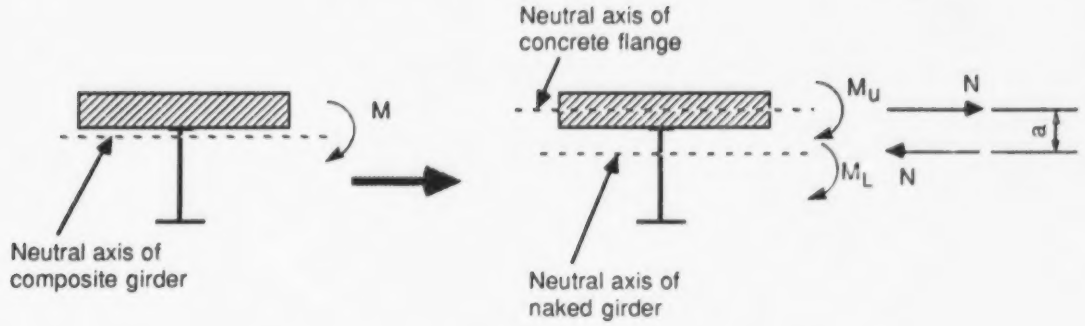

(a) Moments in a Composite Girder

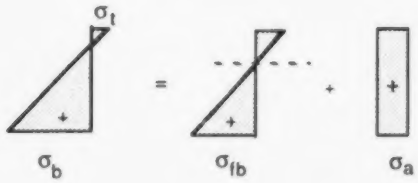

(b) Stresses in the Steel Girder Without Axial Force Due to Bearing Restraint

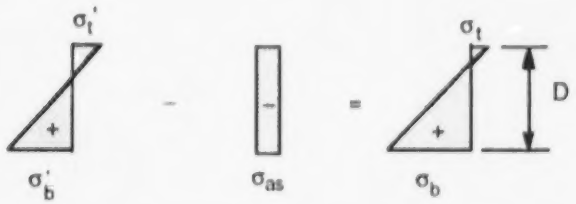

(c) Obtaining Stresses due to Flexure when Axial Force due to Bearing Restraint is Present

Figure 6.3/ Calculation of Girder Moments from Measured Strains

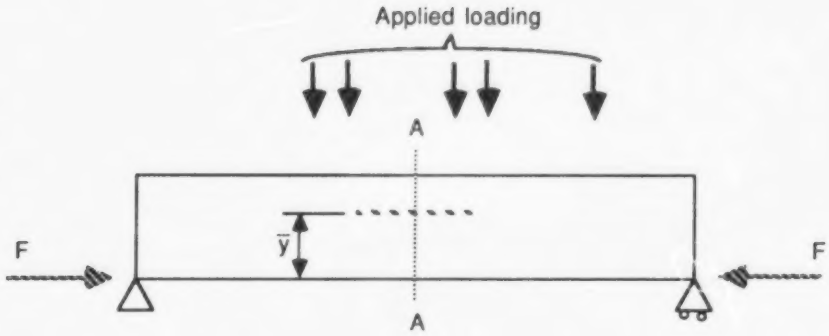

Net moment at section A-A at neutral axis
= Moment due to applied loading $-F\bar{y}$

Figure 6.4/ Reduction of Applied Load Moment Due to Bearing Restraint

$I = 0.0509\ m^4$

$A = 0.0586\ m^2$

$S_b = 0.0523\ m^3$

$E = 2 \times 10^8\ kN/m^2$

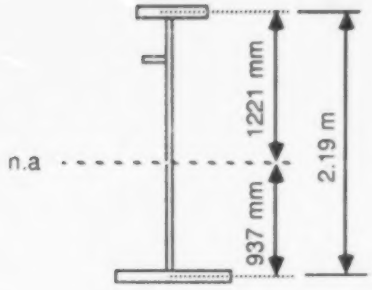

(a) Girder section at mid-span

$A_f = 0.0174\ m^2$

(b) Girder section near support

Figure 6.5/ Girder Section Properties used in the Calculation of Moments

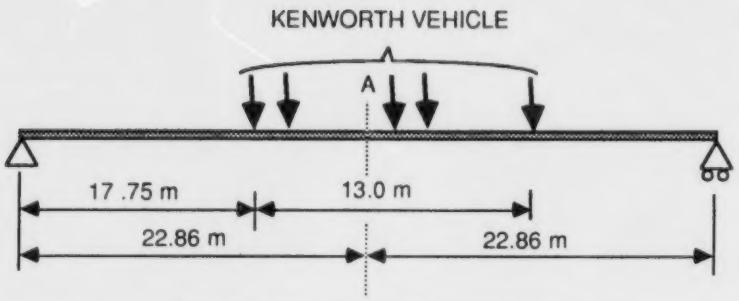

Moment at A due to load level 3 = 6202 kN m
Moment at A due to load level 1 = 4017 kN m

(a) Kenworth vehicle at longitudinal position No.4

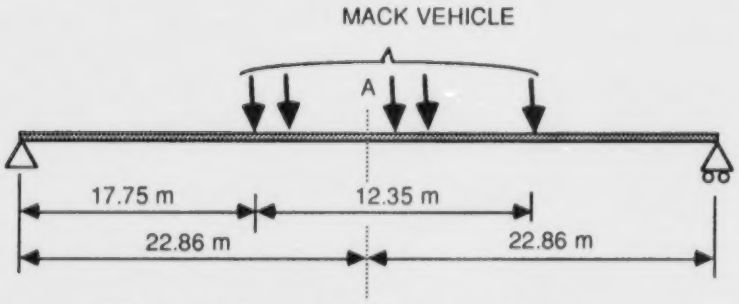

Moment at A due to load level 3 = 6224 kN m
Moment at A due to load level 1 = 4057 kN m

(b) Mack vehicle at longitudinal position No.4

Figure 6.6/ Beam Moments at Mid-Span

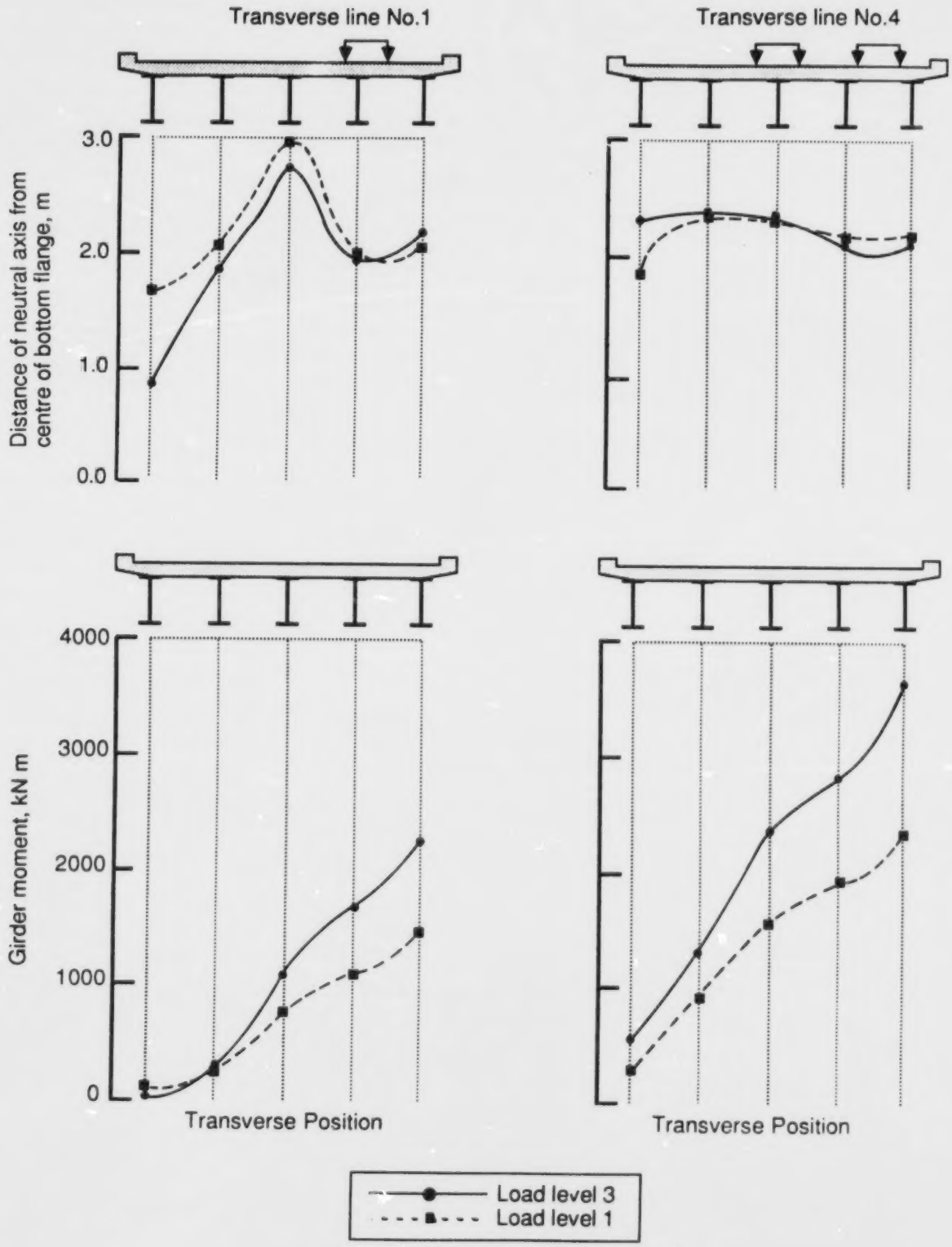

Figure 6.7/ Lateral Distribution of Moments and Neutral Axis Positions due to Vehicles in Longitudinal Position No.4

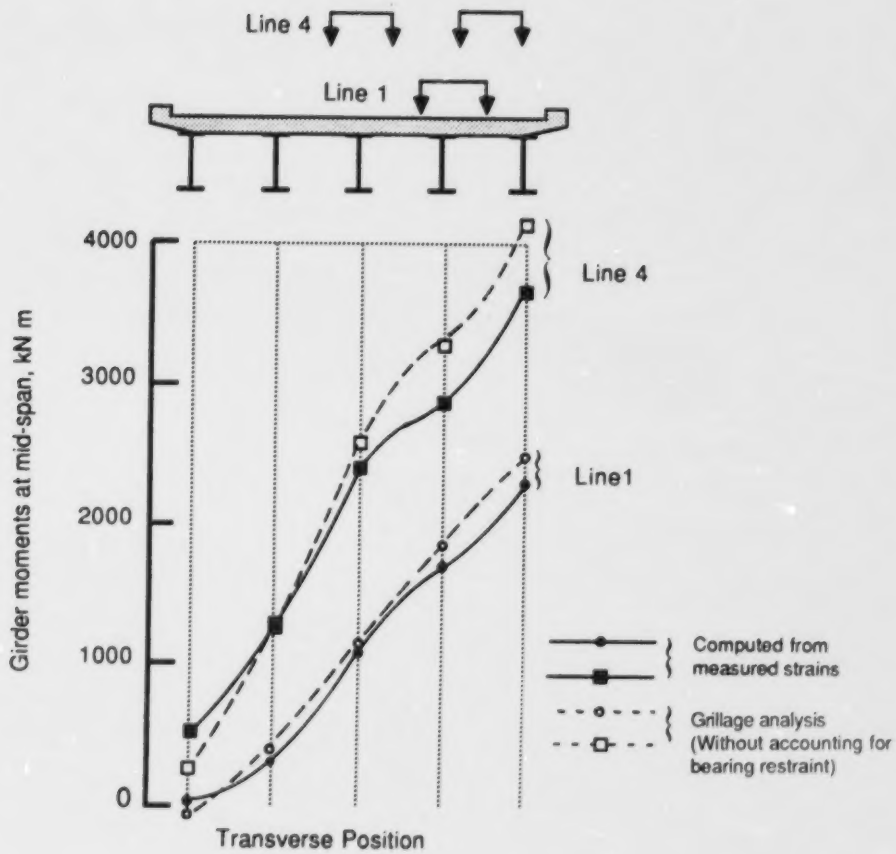

Figure 6.8/ Comparison of Analytical Moments with those Computed from Measured Strains for Vehicles in Longitudinal Position No.4, and with Load Level 3